

Published in final edited form as:

Diabetes. 2016 September ; 65(9): 2784–2794. doi:10.2337/db16-0058.

The Na⁺/glucose co-transporter inhibitor canagliflozin activates AMP-activated protein kinase by inhibiting mitochondrial function and increasing cellular AMP levels

Simon A. Hawley^{1,†}, Rebecca J. Ford^{2,†}, Brennan K. Smith², Graeme J. Gowans¹, Sarah J. Mancini³, Ryan D. Pitt², Emily A. Day², Ian P. Salt³, Gregory R. Steinberg^{2,††}, and D. Grahame Hardie^{1,††}

¹Division of Cell Signalling & Immunology, School of Life Sciences, University of Dundee, Dundee, Scotland, UK

²Division of Endocrinology and Metabolism, Department of Medicine, McMaster University, Hamilton, Ontario, Canada

³Institute of Cardiovascular and Medical Sciences, College of Medical, Veterinary & Life Sciences, University of Glasgow, Glasgow, Scotland, UK

Abstract

Canagliflozin, dapagliflozin and empagliflozin, all recently approved for treatment of Type 2 diabetes, were derived from the natural product phlorizin. They reduce hyperglycemia by inhibiting glucose reuptake by SGLT2 in the kidney, without affecting intestinal glucose uptake by SGLT1. We now report that canagliflozin also activates AMP-activated protein kinase (AMPK), an effect also seen with phloretin (the aglycone breakdown product of phlorizin), but not to any significant extent with dapagliflozin, empagliflozin or phlorizin. AMPK activation occurred at canagliflozin concentrations measured in human plasma in clinical trials, and was caused by inhibition of Complex I of the respiratory chain, leading to increases in cellular AMP or ADP. Although canagliflozin also inhibited cellular glucose uptake independently of SGLT2, this did not account for AMPK activation. Canagliflozin also inhibited lipid synthesis, an effect that was absent in AMPK knockout cells and that required phosphorylation of ACC1 and/or ACC2 at the AMPK sites. Oral administration of canagliflozin activated AMPK in mouse liver, although not in muscle, adipose tissue or spleen. As phosphorylation of acetyl-CoA carboxylase by AMPK is known to lower liver lipid content, these data suggest a potential additional benefit of canagliflozin therapy compared to other SGLT2 inhibitors.

This is an author-created, uncopyedited electronic version of an article accepted for publication in *Diabetes*. The American Diabetes Association (ADA), publisher of *Diabetes*, is not responsible for any errors or omissions in this version of the manuscript or any version derived from it by third parties. The definitive publisher-authenticated version will be available in a future issue of *Diabetes* in print and online at <http://diabetes.diabetesjournals.org>

Corresponding authors: Dr. D. G. Hardie, Division of Cell Signalling & Immunology, School of Life Sciences, University of Dundee, Dow Street, Dundee, DD1 5EH, Scotland, UK; Dr. G.R. Steinberg, Division of Endocrinology and Metabolism, Department of Medicine, McMaster University, Hamilton, Ontario, Canada, Tel: +44 (1382) 384253; FAX: +44 (1382) 385507;

d.g.hardie@dundee.ac.uk, Tel: +1 (905) 525-9140 ext.21691; gsteinberg@mcmaster.ca.

[†]these authors made equal contributions to this study

^{††}joint corresponding authors

A recently introduced approach to treatment of Type 2 diabetes is selective inhibition of sodium/glucose cotransporter-2 (SGLT2) (1). SGLT1 and SGLT2 are related transporters that carry glucose across apical membranes of polarized epithelial cells against concentration gradients, driven by Na⁺ gradients. SGLT1 is expressed in small intestine and responsible for most glucose uptake across the brush border membrane of enterocytes, while SGLT2 is expressed in kidney and responsible for most glucose reabsorption in the convoluted proximal tubules. The first identified SGLT inhibitor was a natural product, phlorizin, which is broken down in the small intestine to the aglycone form, phloretin (Fig. 1). Although phlorizin had beneficial effects in hyperglycemia animals (2), it inhibits both SGLT1 and SGLT2, causing gastrointestinal side-effects (3). This led to development of the synthetic analogs canagliflozin (4), dapagliflozin (5) and empagliflozin (6) (Fig. 1), which have 260-fold, 1100-fold and 2,700-fold selectivity for SGLT2 over SGLT1, respectively (6). In meta-analyses of clinical trials in Type 2 diabetes, canagliflozin (7), dapagliflozin (8) or empagliflozin (9), either as monotherapy or combined with existing therapies, all reduced fasting plasma glucose, HbA1C and body weight, while canagliflozin also decreased plasma triglycerides (7).

The current front-line therapy for Type 2 diabetes is metformin, a biguanide that lowers plasma glucose primarily by reducing hepatic glucose production (10). Metformin, and the related biguanide phenformin, inhibit complex I of the respiratory chain (11; 12), and activate the cellular energy sensor, AMP-activated protein kinase (AMPK) (13; 14). Binding to the AMPK- γ subunit of AMP and/or ADP, which are elevated during cellular energy stress, causes conformational changes that activate the kinase via allosteric effects and promotion of net phosphorylation of Thr172 on the AMPK- α subunit (15–18). Metformin and phenformin increase ADP:ATP ratios, and fail to activate AMPK containing a γ subunit mutant that does not bind AMP/ADP (19), confirming that their AMPK-activating effects are mediated by increases in AMP/ADP. Once activated, AMPK acts to restore energy homeostasis by promoting catabolic pathways including fatty acid oxidation, while inhibiting anabolic pathways including fatty acid synthesis (15; 16). Its opposing acute effects on fat synthesis and oxidation are due to phosphorylation of two acetyl-CoA carboxylase isoforms, ACC1 and ACC2. There has been controversy as to whether AMPK explains all therapeutic benefits of metformin, because its acute effects on hepatic glucose production in mice were reported to be AMPK-independent (20; 21). However, studies using knock-in mice, in which both ACC isoforms were replaced by mutants lacking the critical AMPK phosphorylation sites, suggested that the longer-term insulin-sensitizing effects of metformin are accounted for by phosphorylation and inactivation of ACC1/ACC2 by AMPK (22).

We now report that canagliflozin activates AMPK, in intact cells and in vivo, by a mechanism involving inhibition of respiratory chain Complex I. Our results raise the possibility that some therapeutic benefits of canagliflozin might occur via AMPK activation rather than SGLT2 inhibition.

Research Design and Methods

Materials and antibodies

Canagliflozin, dapagliflozin and empagliflozin were from Selleckchem; phlorizin, phloretin, metformin, phenformin, AICAR and 2-dinitrophenol from Sigma. A769662 was synthesized as described (23). Antibodies against phospho-Thr172 on AMPK- α (pT172, #2531) were from Cell Signaling Technology. In Fig. 8, antibodies against phospho-ACC (pACC, #3661) and total ACC (#3676) were from Cell Signaling Technology. In other Figures, total ACC was detected using streptavidin directly conjugated to 800 nm fluorophore (Rockland immunochemicals), and pACC (14) and total AMPK- α (24) antibodies were as previously described. Anti-GLUT1 (#325510) was from Abcam and anti-SGLT2 (sc-47402) from Santa Cruz.

Cell culture and lysis

HEK-293 cells, and wild type and AMPK knockout mouse embryo fibroblasts (MEFs) (25), were grown in Dulbecco's Modified Eagle's Medium (DMEM) with 25 mmol/l glucose and 10% FBS; cell lysates were prepared as described previously (19). For Western blots shown in Fig. 6C, tissues were homogenised in 5 vols of HES buffer (20 mmol/l Na Hepes, pH 7.4, 250 mmol/l sucrose, 1 mmol/l EDTA, Roche complete protease inhibitor cocktail) with a Dounce homogeniser and centrifuged (7,050 g, 20 min, 4°C). The pellet was resuspended in HES buffer and layered on top of buffer containing 1.12 mol/l sucrose, prior to centrifugation in a swing-out rotor (41,500 g, 60 min, 4°C). Membranes were collected from the interface of the sucrose layers, diluted in HES buffer and centrifuged (150,000 g, 60 min, 4°C). The resultant plasma membrane-rich pellets were resuspended in HES buffer (0.2-0.4 ml).

Immunoprecipitate kinase assays and other analyses

Methods for AMPK assay in immunoprecipitates, SDS-PAGE, Western blotting, and determination of cellular ADP:ATP ratios and oxygen consumption in HEK-293 cells were described previously (19). Lipid synthesis in MEFs was analysed by starving cells of serum for 3 hr then treating with drug or vehicle in the presence of [^{14}C] acetate (1mCi/ml)/0.4 mmol/l Na acetate for 3 hr. Cells washed with PBS prior to extraction to determine incorporation of label into total lipid (26). Fatty acid oxidation was measured as etomoxir-sensitive $^3\text{H}_2\text{O}$ production from [^3H]palmitate. MEFs were preincubated with AMPK activators for 30 min prior to incubation in [^3H]palmitic acid (8 $\mu\text{Ci/ml}$, 110 $\mu\text{mol/l}$), carnitine (50 $\mu\text{mol/l}$), fatty acid-free bovine serum albumin (0.5 mg/mL) in Earle's-Hepes (116 mmol/l NaCl, 5.3 mmol/l KCl, 0.8 mmol/l MgSO_4 , 1.8 mmol/l CaCl_2 , 1 mmol/l NaH_2PO_4 , 20 mmol/l Hepes-NaOH, pH 7.4) in the presence or absence of etomoxir (50 $\mu\text{mol/l}$) for 90 min at 37°C; $^3\text{H}_2\text{O}$ generated was separated and quantified as described (27).

Animal experiments

All animal procedures were approved by the McMaster University Animal Ethics Research Board. Male and female mice (16-20 week), either wild-type or ACC1/ACC2 (S79A/S212A) double knock-in (DKI), were housed in a pathogen-free facility under a 12 hr light/

dark cycle at 23°C, with *ad libitum* access to standard chow and water. Primary hepatocytes were generated from wild type and DKI mice and the following day were treated for 4 hr with canagliflozin or vehicle before assessing AMPK and ACC phosphorylation and lipid synthesis, as described (22; 28). For experiments to examine AMPK and ACC phosphorylation *in vivo*, canagliflozin or vehicle (saline solution containing 0.5% carboxymethyl cellulose, 0.025% Tween-20) was administered by oral gavage (100 mg/kg, 10 µl/g). Mice were anaesthetized and tissues snap frozen *in situ* as previously described (22). Measurements of respiratory exchange ratio were performed in metabolic cages using a protocol (29) in which mice were fasted overnight and refed with chow for 2 hr before being gavaged with canagliflozin or vehicle as the time of food withdrawal. In separate experiments, mice were treated as above, blood collected from a nick in the tail and glucose measured using a Roche glucometer.

Measurements of oxygen uptake/respiration in primary mouse hepatocytes

Mitochondrial respiration was measured by high-resolution respirometry (Oroboros Oxygraph-2 k, Innsbruck, Austria) at 37°C and room air-saturated O₂ tension in respiration buffer (MIRO5) containing EGTA (0.5 mmol/l), MgCl₂ (3 mmol/l), K-lactobionate (60 mmol/l), KH₂PO₄ (10 mmol/l), HEPES (20 mmol/l), sucrose (110 mmol/l) and fatty acid free BSA (1 g/l). Primary hepatocytes from wild type mice were generated as described above. The following day they were suspended in 2 ml of respiration buffer and 800 µl of the suspension added to respiration chambers. Digitonin (8.1 µmol/l) was added to permeabilize the cells, and 5 min later the assay was initiated. To measure Complex I-supported respiration, glutamate (5 mmol/l), malate (2 mmol/l) and ADP (2.5 mmol/l) were added and respiration allowed to reach steady state. To measure Complex II-supported respiration, rotenone (1.25 µmol/l), succinate (10 mmol/l) and ADP (2.5 mmol/l) were added and respiration allowed to reach steady state. Drugs were then added to respiring cells at the indicated concentrations.

Measurements of glucose uptake

Cells were incubated in glucose-free Krebs-Ringer phosphate for 2 hr, with AICAR present for the last 1 hr or canagliflozin/dapagliflozin for the last 15 min. 2-deoxyglucose (50 µmol/l, 1µCi/ml) was added and cytochalasin B-sensitive 2-deoxyglucose uptake was measured over 10 min (30).

Statistical analysis

Significance of differences was assessed using student's t test, 1-way or 2-way ANOVA as appropriate, using Sidak's test after ANOVA. Significance is indicated in Figures as follows: **P*<0.05, ***P*<0.01, ****P*<0.001, *****P*<0.0001 or †*P*<0.05, ††*P*<0.01, †††*P*<0.001, ††††*P*<0.0001.

Results

Canagliflozin and phloretin, but not dapagliflozin, empagliflozin or phlorizin, significantly activate AMPK in HEK-293 cells

To assess the impact of canagliflozin on AMPK, we initially utilized HEK-293 cells. A daily 300 mg dose of canagliflozin produces a peak plasma concentration in humans of around 10 $\mu\text{mol/l}$ (31), so we tested concentrations from 1 to 30 $\mu\text{mol/l}$. Following incubation for 1 hour (Fig. 2A), canagliflozin increased AMPK activity at concentrations from 1-30 $\mu\text{mol/l}$, with 10 $\mu\text{mol/l}$ giving a similar activation to that observed with 300 $\mu\text{mol/l}$ A769662 (which activates AMPK by direct binding between the α and β subunits (32)) or berberine (a mitochondrial inhibitor that activates AMPK by increasing cellular AMP:ATP (19)). AMPK activation by canagliflozin, A769662 and berberine was associated with increased phosphorylation of Thr172 on AMPK and of the primary AMPK site on ACC (pACC) (Fig. 2A; quantified results shown in Figs. S1A/B in Supplementary Data). Fig. 2B shows that the effect of 30 $\mu\text{mol/l}$ canagliflozin was rapid, reaching a maximum by 20 minutes.

Figs. 2C/D compare the effects of canagliflozin, dapagliflozin and empagliflozin. Although both of the latter activated AMPK, this required concentrations >30 $\mu\text{mol/l}$, and even at 100 $\mu\text{mol/l}$ their effects were small compared with canagliflozin. Effects on phosphorylation of AMPK and ACC (Figs. 2F-H, quantified results in Figs. S1C-F) were consistent with this. Since single doses of dapagliflozin (20 mg) or empagliflozin (50 mg) produce peak plasma concentrations of only 1-2 $\mu\text{mol/l}$ (33; 34), it seems unlikely that these inhibitors would produce significant AMPK activation at normal therapeutic doses.

We also examined the effects of the natural product phlorizin and its aglycone form, phloretin. Interestingly, phloretin activated AMPK, and promoted phosphorylation of AMPK and ACC, at concentrations slightly higher than canagliflozin. However, phlorizin only affected these parameters marginally at much higher concentrations (Figs. 2E/I/J; quantification of blots in Fig. S1G/H).

Canagliflozin activates AMPK by inhibiting Complex I of the respiratory chain

To test whether canagliflozin activated AMPK by increasing cellular AMP or ADP, we tested its effects in HEK-293 cells expressing the wild type AMPK- γ 2 subunit (WT cells) or the AMP/ADP-insensitive R531G mutant (RG cells) (19). Canagliflozin activated AMPK and promoted its phosphorylation in WT cells, but not in RG cells; similar results were obtained with phloretin (Fig. 3; quantification of blots in Fig. S2). These results suggest that canagliflozin and phloretin activate AMPK by increasing cellular AMP or ADP.

Cellular AMP levels are low and difficult to measure in cultured cells, so we routinely measure ADP:ATP ratios as a surrogate for AMP:ATP (17). Increasing concentrations of canagliflozin caused increases in ADP:ATP ratio that were significant at 10 and 30 $\mu\text{mol/l}$, with 30 $\mu\text{mol/l}$ canagliflozin producing an effect similar to 10 mmol/l phenformin (Fig. 4A). Similar results were obtained with phloretin (Fig. 4B). The increase in cellular ADP:ATP due to canagliflozin was accompanied by reduction of cellular oxygen consumption (Fig. 4C); the effect of 30 $\mu\text{mol/l}$ canagliflozin was smaller, although more rapid, than that of 10 mmol/l phenformin. When the uncoupler 2,4-dinitrophenol (DNP) was added 60 minutes

later, in cells treated with DMSO there was a large increase in oxygen consumption (representing the maximal respiration rate when mitochondria were not limited by the supply of ADP). However, as canagliflozin concentrations increased the effects of DNP were eliminated suggesting that, like phenformin, canagliflozin inhibited the respiratory chain rather than the F1 ATP synthase.

We next used primary mouse hepatocytes permeabilised with digitonin, and measured the function of respiratory chain Complexes I and II. Fig. 4D and E show that canagliflozin and dapagliflozin inhibited Complex I-supported respiration in a concentration-dependent manner, whereas any effect on Complex II was marginal. The inhibitory effect of canagliflozin on Complex I was significantly greater than that of dapagliflozin, with estimated half-maximal effects at $18 \pm 1 \mu\text{mol/l}$ for canagliflozin and $40 \pm 3 \mu\text{mol/l}$ for dapagliflozin.

AMPK-dependent and –independent effects of canagliflozin on cellular metabolism

To examine effects of canagliflozin on metabolic effects mediated by AMPK, we initially used immortalized MEFs with a double knockout of AMPK- $\alpha 1$ and - $\alpha 2$ (DKO), or wild type controls. Fig. 5A shows that AMPK was activated by concentrations of canagliflozin above $1 \mu\text{mol/l}$ in WT cells, associated with phosphorylation of AMPK and ACC (blots quantified in Fig. S3A/B). As expected, AMPK activity was undetectable in DKO cells, and although ACC expression was normal there was no basal or canagliflozin-stimulated ACC phosphorylation. We next measured lipid synthesis using [^{14}C]acetate, and fatty acid oxidation using [^3H]palmitate (Figs. 5B/C). A769662 and phenformin (which activate AMPK by different mechanisms) caused inhibition of lipid synthesis in the WT cells, while canagliflozin caused increasing inhibition at 10 and $30 \mu\text{mol/l}$. As expected, the inhibition by A769662 was abolished in DKO cells but, surprisingly, lipid synthesis was *stimulated* by both phenformin and canagliflozin in DKO cells. Fatty acid oxidation (Fig 5C) was stimulated by AICAR and this was abolished in the DKO cells, showing that it was AMPK-dependent. However, phenformin and canagliflozin inhibited fatty acid oxidation in both the WT and DKO cells. The explanation for this is likely to be that these drugs, although activating AMPK, inhibit the respiratory chain and therefore prevent re-oxidation of NADH and FADH_2 generated by fat oxidation, an effect that would be AMPK-independent, and that has been observed previously in primary hepatocytes treated with metformin (22).

Canagliflozin inhibits lipogenesis in hepatocytes through a mechanism involving phosphorylation of ACC by AMPK

The inhibition of lipid synthesis by canagliflozin in Fig. 5B was associated with phosphorylation of ACC at the AMPK site(s) (Fig. 5A, results quantified in Fig. S3B). To test whether the effect of canagliflozin on lipid synthesis required phosphorylation of ACC1/ACC2, we studied hepatocytes from mice with a double knock-in (DKI) of mutations at the AMPK sites on both ACC isoforms (22). Fig. 5D shows that increasing concentrations of canagliflozin caused progressive inhibition of lipid synthesis in WT hepatocytes that was abolished, at least at concentrations of $10 \mu\text{mol/l}$ and below, in DKI cells. The effects of $500 \mu\text{mol/l}$ metformin were also abolished in the DKI cells. However, at $30 \mu\text{mol/l}$ canagliflozin there was still some inhibition in the DKI cells, although significantly less than in WT cells.

The effects of canagliflozin and metformin on lipid synthesis were accompanied by increased phosphorylation of AMPK and, in WT cells, of ACC. The pACC and total ACC antibodies both detected doublets; the lower and upper bands are ACC1 (predicted mass 265 kDa) and ACC2 (276 kDa) (22). Fig. 5E shows that 10-30 $\mu\text{mol/l}$ canagliflozin significantly increased pT172/AMPK- α and pACC/ACC (ACC1 + ACC2) in wild type mouse hepatocytes.

Canagliflozin inhibits glucose uptake in HEK-293 cells and MEFs

We next assessed the effects of the drugs on glucose transport by measuring 2-deoxyglucose (2DG) uptake. Canagliflozin inhibited uptake by 50-60% in both HEK-293 cells and MEFs, whereas the AMPK activator AICAR had no effect. The results were identical in wild type MEFs and AMPK DKO MEFs, showing that this effect of canagliflozin was AMPK-independent. We also assessed the expression of SGLT2 in these cell types using Western blotting. HEK-293 cells and mouse liver, but not MEFs, expressed a polypeptide that co-migrated with SGLT2 in mouse kidney. HEK-293 cells, MEFs and mouse liver also appeared to express GLUT1, although the band did not always co-migrate with the bands in control tissue, possibly due to variable glycosylation (Fig. 6C). Attempts to measure expression of other glucose transporters (GLUT3, SGLT1) by Western blotting were inconclusive. The effect of canagliflozin to inhibit glucose uptake in HEK-293 cells and MEFs appears to be yet another off-target effect, because dapagliflozin had no effect on 2DG uptake in either cell type (Fig. 6A/B). To further confirm that the activation of AMPK in HEK-293 cells was not secondary to its effects on glucose uptake, we compared the effects of canagliflozin with complete glucose removal from the medium (Fig. 6D; quantification of blots in Fig. S3C/D). While removal of all glucose caused a modest activation and Thr172 phosphorylation of AMPK, activation by 30 $\mu\text{mol/l}$ canagliflozin was >3-fold larger. Since inhibition of glucose uptake by canagliflozin was only partial (Fig. 6A), the effect of canagliflozin on AMPK is unlikely to be due to reduced supply of glucose for catabolism.

Canagliflozin activates AMPK in mice in vivo

To test whether canagliflozin activated AMPK in vivo, it was administered to mice (100 mg/kg) by oral gavage, and 3 hr later tissues were collected by freeze clamping in situ, which preserves the activation state of AMPK (35). In liver, Thr172 phosphorylation of AMPK was significantly increased by this treatment, as was the phosphorylation of ACC and Raptor at AMPK sites (Figs. 7A, S4). By contrast, significant increases in phosphorylation of AMPK, ACC and Raptor were not observed in muscle (tibialis anterior), gonadal white adipose tissue or spleen (Fig. S5A-C). We also measured the effects of oral administration of canagliflozin, administered at the time of withdrawing food from previously fasted mice that had been refed for 2 hr, on respiratory exchange ratio (RER). In WT mice canagliflozin caused a more rapid drop in RER than vehicle, indicating a more rapid shift back towards fat rather than carbohydrate oxidation (Fig 7B). However, this was also observed in ACC1/ACC2 DKI mice, showing that the effect was independent of ACC phosphorylation and therefore presumably of AMPK (Fig 7C). This reduction in RER by canagliflozin was likely secondary to reduction of blood glucose, which was similar in both WT and ACC DKI mice (Fig 7D).

Discussion

Recent clinical trials suggest that the SGLT2 inhibitors canagliflozin, dapagliflozin and empagliflozin show promise for reversal of hyperglycemia, either as monotherapy or as adjuncts to existing therapy. Compared with dapagliflozin, canagliflozin also has consistently favorable effects on plasma lipid profiles (7; 8; 36; 37). These differential effects on plasma lipids prompted us to investigate whether canagliflozin might have SGLT2-independent effects. Our results show that canagliflozin causes a substantial activation of AMPK in both human and mouse cells, at concentrations corresponding to the peak plasma concentrations achieved following therapeutic doses in humans. By contrast, dapagliflozin and empagliflozin only caused a modest AMPK activation at concentrations well above their peak plasma concentrations. Thus, activation of AMPK by dapagliflozin or empagliflozin is less likely to be significant in vivo.

Our results demonstrate that AMPK activation is primarily due to inhibition of Complex I of the respiratory chain, leading to increases in cellular AMP/ADP that bind to the γ subunit and promote Thr172 phosphorylation. Thus, canagliflozin: (i) increased cellular ADP:ATP ratios; (ii) increased AMPK activation and Thr172 phosphorylation in cells expressing the wild type but not the AMP/ADP-insensitive R531G mutant of AMPK- γ 2; (iii) inhibited oxygen uptake in HEK-293 cells; (iv) inhibited oxygen uptake in permeabilized mouse hepatocytes provided with substrates that feed into complex I. Dapagliflozin also caused a less potent effect on Complex I, although only at concentrations (10-30 μ mol/l) higher than those observed in human plasma with normal doses. We also found that canagliflozin, but not dapagliflozin, inhibited 2-deoxyglucose uptake in HEK-293 cells and MEFs in an AMPK-independent manner, indicating that it had additional off-target effects on glucose transport, presumably due to inhibition of another glucose transporter such as GLUT1. Indeed, previous studies in L6 myotubes have indicated that 10 μ mol/l canagliflozin can inhibit glucose uptake by approximately 50%, an effect that was attributed to GLUT1 inhibition (38). However, this is unlikely to account for the AMPK activation observed in our experiments, because even complete removal of glucose from the medium had only a modest effect on AMPK activity compared to canagliflozin.

Interestingly, we found that the aglycone derivative of phlorizin, phloretin, also activated AMPK, although phlorizin itself was much less effective. Like canagliflozin, phloretin appeared to act by increasing cellular AMP. Both phlorizin (39) and phloretin (40) were reported previously to inhibit the function of isolated mitochondria, but we found that only phloretin is effective in intact cells, perhaps due to greater membrane permeability.

Our studies also show that AMPK activation has the expected effects on lipid synthesis in intact cells. Thus, three distinct AMPK activators, A769662, phenformin and canagliflozin, all inhibited the pathway in MEFs, and these inhibitory effects were abolished in MEFs lacking AMPK, correlating with a complete loss of ACC phosphorylation. Surprisingly, phenformin and canagliflozin (but not A769662) *stimulated* lipid synthesis in DKO cells. When we measured fatty acid oxidation in the same cells, phenformin and canagliflozin inhibited the pathway in an AMPK-independent manner, which is expected since both compounds inhibit Complex I. The major fates of cellular acetyl-CoA are oxidation by the

TCA cycle or incorporation into lipids. Thus, in the absence of AMPK to inhibit lipid synthesis, acetate flux might be diverted into lipid synthesis as oxidation was inhibited. This provides an explanation for the paradoxical activation of lipid synthesis by phenformin and canagliflozin observed in AMPK knockout cells.

Our results in isolated mouse hepatocytes demonstrate that the effects of canagliflozin on lipid synthesis are mediated by phosphorylation of ACC. Thus, a moderate and therapeutically relevant concentration of canagliflozin (10 $\mu\text{mol/l}$) inhibited lipid synthesis in WT hepatocytes, but failed to do so in DKI cells from mice where both ACC isoforms lacked the critical AMPK site. At higher canagliflozin (30 $\mu\text{mol/l}$) there was some inhibition even in DKI hepatocytes, although significantly less than in WT cells; this is most likely because both ACC isoforms use ATP as a direct substrate. Once the increase in cellular ADP:ATP ratio becomes substantial, as with 30 $\mu\text{mol/l}$ canagliflozin (Fig. 4A), decreases in ATP may limit flux through ACC independently of AMPK. This is a revealing demonstration of the physiological role of AMPK: as ATP falls under situations of energetic stress the kinase limits the function of energy-consuming pathways *before* the ATP concentration has dropped to levels where it becomes limiting for the pathway itself. This occurs because AMPK is more sensitive to ATP depletion than the ATP-consuming enzymes in the pathway.

Our results show that oral administration of canagliflozin increased Thr172 phosphorylation of AMPK in liver in vivo, as well as phosphorylation of two of its well-recognized downstream targets, ACC and Raptor. Although we only tested effects of the drug in normal mice, there is no reason to believe the results would be any different in diabetic models. For example, berberine (which activates AMPK by the same mechanism as canagliflozin (19)) activates AMPK normally in db/db mice (42). Canagliflozin also caused a more rapid drop in respiratory exchange ratio when administered to fed mice, indicating a more rapid switch to fat versus carbohydrate oxidation. However, this was still observed in the DKI mice, and was therefore presumably independent of AMPK. It is possible that a reduction in blood glucose caused by canagliflozin causes increased fat oxidation due to competition between glucose and fat for substrate oxidation (41), and that this obscures any effect due to ACC phosphorylation by AMPK; this might be addressed in future studies using SGLT2 knockout mice.

Our findings raise the interesting question as to whether dual therapy with canagliflozin and metformin would be more effective than canagliflozin alone. In a recently reported clinical trial of newly diagnosed subjects with type 2 diabetes (43), monotherapy with canagliflozin was found to be more effective in lowering HBA1C than metformin. Although dual therapy was more efficacious than canagliflozin alone, the effects of the two drugs were not additive, as might be expected if they had distinct mechanisms of action. By contrast, in a similar trial using metformin and dapagliflozin, monotherapy with dapagliflozin was not more effective than metformin, and the effects of dual therapy were closer to being additive (44).

Finally, although the long-term effects of metformin to inhibit hepatic glucose production in mice are AMPK-dependent (22), studies have suggested that its rapid effects are AMPK-independent (20; 21). However, the latter authors agree that the primary effect of metformin

is to inhibit the respiratory chain and increase cellular AMP in the liver, which is then proposed to affect other AMP-sensitive targets such as fructose-1,6-bisphosphatase (20) or adenylate cyclase (21). Since canagliflozin inhibits the respiratory chain and activates AMPK in liver, it is conceivable that these AMP-dependent, but AMPK-independent, effects of metformin might also be mimicked by canagliflozin.

Supplementary Material

Refer to Web version on PubMed Central for supplementary material.

Acknowledgements

Author contributions: SAH, RJF, BKS, GJG, SJM, RDP and EAD established experimental protocols and/or conducted experiments, while IPS, GRS and DGH supervised research. DGH and GRS wrote the initial manuscript, while all authors contributed revisions and corrections. None of the authors have a conflict of interest with the content of this paper.

DGH and GRS are the guarantors of this work, have had full access to all the data in the study and takes responsibility for the integrity of the data and the accuracy of the data analysis. The study was supported by a Senior Investigator Award from the Wellcome Trust [097726, to DGH], by the pharmaceutical companies supporting the Division of Signal Transduction Therapy at Dundee (AstraZeneca, Boehringer-Ingelheim, GlaxoSmithKline, Merck KgaA, Janssen Pharmaceutica and Pfizer), by the Canadian Diabetes Association (GRS) and the Canadian Institutes of Health Research (GRS). GRS is a Canada Research Chair in Metabolism and Obesity and the J. Bruce Duncan Chair in Metabolic Diseases. SJM and IPS were supported by a Project Grant (PG/13/82/30483) from the British Heart Foundation. We thank Benoit Viollet for AMPK knockout MEFs.

References

- Rosenwasser RF, Sultan S, Sutton D, Choksi R, Epstein BJ. SGLT-2 inhibitors and their potential in the treatment of diabetes. *Diabetes, metabolic syndrome and obesity : targets and therapy*. 2013; 6:453–467.
- Rossetti L, Smith D, Shulman GI, Papachristou D, DeFronzo RA. Correction of hyperglycemia with phlorizin normalizes tissue sensitivity to insulin in diabetic rats. *J Clin Invest*. 1987; 79:1510–1515. [PubMed: 3571496]
- Ehrenkranz JR, Lewis NG, Kahn CR, Roth J. Phlorizin: a review. *Diabetes Metab Res Rev*. 2005; 21:31–38. [PubMed: 15624123]
- Nomura S, Sakamaki S, Hongu M, Kawanishi E, Koga Y, Sakamoto T, Yamamoto Y, Ueta K, Kimata H, Nakayama K, Tsuda-Tsukimoto M. Discovery of canagliflozin, a novel C-glucoside with thiophene ring, as sodium-dependent glucose cotransporter 2 inhibitor for the treatment of type 2 diabetes mellitus. *J Med Chem*. 2010; 53:6355–6360. [PubMed: 20690635]
- Meng W, Ellsworth BA, Nirschl AA, McCann PJ, Patel M, Girotra RN, Wu G, Sher PM, Morrison EP, Biller SA, Zahler R, et al. Discovery of dapagliflozin: a potent, selective renal sodium-dependent glucose cotransporter 2 (SGLT2) inhibitor for the treatment of type 2 diabetes. *J Med Chem*. 2008; 51:1145–1149. [PubMed: 18260618]
- Grempler R, Thomas L, Eckhardt M, Himmelsbach F, Sauer A, Sharp DE, Bakker RA, Mark M, Klein T, Eickelmann P. Empagliflozin, a novel selective sodium glucose cotransporter-2 (SGLT-2) inhibitor: characterisation and comparison with other SGLT-2 inhibitors. *Diabetes Obes Metab*. 2012; 14:83–90. [PubMed: 21985634]
- Yang XP, Lai D, Zhong XY, Shen HP, Huang YL. Efficacy and safety of canagliflozin in subjects with type 2 diabetes: systematic review and meta-analysis. *Eur J Clin Pharmacol*. 2014; 70:1149–1158. [PubMed: 25124541]
- Sun YN, Zhou Y, Chen X, Che WS, Leung SW. The efficacy of dapagliflozin combined with hypoglycaemic drugs in treating type 2 diabetes mellitus: meta-analysis of randomised controlled trials. *BMJ open*. 2014; 4:e004619.

9. Liakos A, Karagiannis T, Athanasiadou E, Sarigianni M, Mainou M, Papatheodorou K, Bekiari E, Tsapas A. Efficacy and safety of empagliflozin for type 2 diabetes: a systematic review and meta-analysis. *Diabetes Obes Metab.* 2014; 16:984–993. [PubMed: 24766495]
10. Natali A, Ferrannini E. Effects of metformin and thiazolidinediones on suppression of hepatic glucose production and stimulation of glucose uptake in type 2 diabetes: a systematic review. *Diabetologia.* 2006; 49:434–441. [PubMed: 16477438]
11. Owen MR, Doran E, Halestrap AP. Evidence that metformin exerts its anti-diabetic effects through inhibition of complex 1 of the mitochondrial respiratory chain. *Biochem J.* 2000; 348:607–614. [PubMed: 10839993]
12. El-Mir MY, Nogueira V, Fontaine E, Averet N, Rigoulet M, Leverve X. Dimethylbiguanide inhibits cell respiration via an indirect effect targeted on the respiratory chain complex I. *J Biol Chem.* 2000; 275:223–228. [PubMed: 10617608]
13. Zhou G, Myers R, Li Y, Chen Y, Shen X, Fenyk-Melody J, Wu M, Ventre J, Doebber T, Fujii N, Musi N, et al. Role of AMP-activated protein kinase in mechanism of metformin action. *J Clin Invest.* 2001; 108:1167–1174. [PubMed: 11602624]
14. Hawley SA, Boudeau J, Reid JL, Mustard KJ, Udd L, Makela TP, Alessi DR, Hardie DG. Complexes between the LKB1 tumor suppressor, STRADa/b and MO25a/b are upstream kinases in the AMP-activated protein kinase cascade. *J Biol.* 2003; 2:28. [PubMed: 14511394]
15. Hardie DG. AMPK--sensing energy while talking to other signaling pathways. *Cell Metab.* 2014; 20:939–952. [PubMed: 25448702]
16. Hardie DG, Schaffer B, Brunet A. AMP-activated protein kinase: an energy-sensing pathway with multiple inputs and outputs. *Trends Cell Biol.* 2015 in press.
17. Gowans GJ, Hawley SA, Ross FA, Hardie DG. AMP is a true physiological regulator of AMP-activated protein kinase by both allosteric activation and enhancing net phosphorylation. *Cell Metab.* 2013; 18:556–566. [PubMed: 24093679]
18. Ross FA, Jensen TE, Hardie DG. Differential regulation by AMP and ADP of AMPK complexes containing different gamma subunit isoforms. *Biochem J.* 2016; 473:189–199. [PubMed: 26542978]
19. Hawley SA, Ross FA, Chevtzoff C, Green KA, Evans A, Fogarty S, Towler MC, Brown LJ, Ogunbayo OA, Evans AM, Hardie DG. Use of cells expressing gamma subunit variants to identify diverse mechanisms of AMPK activation. *Cell Metab.* 2010; 11:554–565. [PubMed: 20519126]
20. Foretz M, Hebrard S, Leclerc J, Zarrinpashneh E, Soty M, Mithieux G, Sakamoto K, Andreelli F, Viollet B. Metformin inhibits hepatic gluconeogenesis in mice independently of the LKB1/AMPK pathway via a decrease in hepatic energy state. *J Clin Invest.* 2010; 120:2355–2369. [PubMed: 20577053]
21. Miller RA, Chu Q, Xie J, Foretz M, Viollet B, Birnbaum MJ. Biguanides suppress hepatic glucagon signalling by decreasing production of cyclic AMP. *Nature.* 2013; 494:256–260. [PubMed: 23292513]
22. Fullerton MD, Galic S, Marcinko K, Sikkema S, Pulinilkunnil T, Chen ZP, O'Neill HM, Ford RJ, Palanivel R, O'Brien M, Hardie DG, et al. Single phosphorylation sites in ACC1 and ACC2 regulate lipid homeostasis and the insulin-sensitizing effects of metformin. *Nat Med.* 2013; 19:1649–1654. [PubMed: 24185692]
23. Goransson O, McBride A, Hawley SA, Ross FA, Shpiro N, Foretz M, Viollet B, Hardie DG, Sakamoto K. Mechanism of action of A-769662, a valuable tool for activation of AMP-activated protein kinase. *J Biol Chem.* 2007; 282:32549–32560. [PubMed: 17855357]
24. Woods A, Salt I, Scott J, Hardie DG, Carling D. The alpha1 and alpha2 isoforms of the AMP-activated protein kinase have similar activities in rat liver but exhibit differences in substrate specificity in vitro. *FEBS Lett.* 1996; 397:347–351. [PubMed: 8955377]
25. Laderoute KR, Amin K, Calaoagan JM, Knapp M, Le T, Orduna J, Foretz M, Viollet B. 5'-AMP-activated protein kinase (AMPK) is induced by low-oxygen and glucose deprivation conditions found in solid-tumor microenvironments. *Mol Cell Biol.* 2006; 26:5336–5347. [PubMed: 16809770]
26. Corton JM, Gillespie JG, Hardie DG. Role of the AMP-activated protein kinase in the cellular stress response. *Curr Biol.* 1994; 4:315–324. [PubMed: 7922340]

27. Reihill JA, Ewart MA, Salt IP. The role of AMP-activated protein kinase in the functional effects of vascular endothelial growth factor-A and -B in human aortic endothelial cells. *Vasc Cell*. 2011; 3:9. [PubMed: 21507243]
28. Davies SP, Carling D, Hardie DG. Tissue distribution of the AMP-activated protein kinase, and lack of activation by cyclic-AMP-dependent protein kinase, studied using a specific and sensitive peptide assay. *Eur J Biochem*. 1989; 186:123–128. [PubMed: 2574667]
29. Hawley SA, Fullerton MD, Ross FA, Schertzer JD, Chevtzoff C, Walker KJ, Peggie MW, Zibrova D, Green KA, Mustard KJ, Kemp BE, et al. The ancient drug salicylate directly activates AMP-activated protein kinase. *Science*. 2012; 336:918–922. [PubMed: 22517326]
30. Salt IP, Connell JM, Gould GW. 5-aminoimidazole-4-carboxamide ribonucleoside (AICAR) inhibits insulin-stimulated glucose transport in 3T3-L1 adipocytes. *Diabetes*. 2000; 49:1649–1656. [PubMed: 11016448]
31. Devineni D, Curtin CR, Polidori D, Gutierrez MJ, Murphy J, Rusch S, Rothenberg PL. Pharmacokinetics and pharmacodynamics of canagliflozin, a sodium glucose co-transporter 2 inhibitor, in subjects with type 2 diabetes mellitus. *J Clin Pharmacol*. 2013; 53:601–610. [PubMed: 23670707]
32. Xiao B, Sanders MJ, Carmena D, Bright NJ, Haire LF, Underwood E, Patel BR, Heath RB, Walker PA, Hallen S, Giordanetto F, et al. Structural basis of AMPK regulation by small molecule activators. *Nature Commun*. 2013; 4:3017. [PubMed: 24352254]
33. Kasichayanula S, Chang M, Hasegawa M, Liu X, Yamahira N, LaCreta FP, Imai Y, Boulton DW. Pharmacokinetics and pharmacodynamics of dapagliflozin, a novel selective inhibitor of sodium-glucose co-transporter type 2, in Japanese subjects without and with type 2 diabetes mellitus. *Diabetes Obes Metab*. 2011; 13:357–365. [PubMed: 21226818]
34. Brand T, Macha S, Mattheus M, Pinnetti S, Woerle HJ. Pharmacokinetics of empagliflozin, a sodium glucose cotransporter-2 (SGLT-2) inhibitor, coadministered with sitagliptin in healthy volunteers. *Adv Ther*. 2012; 29:889–899. [PubMed: 23054692]
35. Davies SP, Carling D, Munday MR, Hardie DG. Diurnal rhythm of phosphorylation of rat liver acetyl-CoA carboxylase by the AMP-activated protein kinase, demonstrated using freeze-clamping. Effects of high fat diets. *Eur J Biochem*. 1992; 203:615–623. [PubMed: 1346520]
36. Bailey CJ, Iqbal N, T'Joel C, List JF. Dapagliflozin monotherapy in drug-naive patients with diabetes: a randomized-controlled trial of low-dose range. *Diabetes Obes Metab*. 2012; 14:951–959. [PubMed: 22776824]
37. Kaku K, Kiyosue A, Inoue S, Ueda N, Tokudome T, Yang J, Langkilde AM. Efficacy and safety of dapagliflozin monotherapy in Japanese patients with type 2 diabetes inadequately controlled by diet and exercise. *Diabetes Obes Metab*. 2014; 16:1102–1110. [PubMed: 24909293]
38. Liang Y, Arakawa K, Ueta K, Matsushita Y, Kuriyama C, Martin T, Du F, Liu Y, Xu J, Conway B, Conway J, et al. Effect of canagliflozin on renal threshold for glucose, glycemia, and body weight in normal and diabetic animal models. *PLoS One*. 2012; 7:e30555. [PubMed: 22355316]
39. Keller DM, Lotspeich WD. Some effects of phlorizin on the metabolism of mitochondria. *J Biol Chem*. 1959; 234:987–990. [PubMed: 13654304]
40. De Jonge PC, Wieringa T, Van Putten JP, Krans HM, Van Dam K. Phloretin - an uncoupler and an inhibitor of mitochondrial oxidative phosphorylation. *Biochim Biophys Acta*. 1983; 722:219–225. [PubMed: 6130789]
41. Randle PJ, Garland PB, Hales CN, Newsholme EA. The glucose fatty-acid cycle. Its role in insulin sensitivity and the metabolic disturbances of diabetes mellitus. *Lancet*. 1963; 1:785–789. [PubMed: 13990765]
42. Kim WS, Lee YS, Cha SH, Jeong HW, Choe SS, Lee MR, Oh GT, Park HS, Lee KU, Lane MD, Kim JB. Berberine improves lipid dysregulation in obesity by controlling central and peripheral AMPK activity. *Am J Physiol Endocrinol Metab*. 2009; 296:E812–E819. [PubMed: 19176354]
43. Rosenstock J, Chuck L, Gonzalez-Ortiz M, Merton K, Craig J, Capuano G, Qiu R. Initial combination therapy with canagliflozin plus metformin versus each component as monotherapy for drug-naive type 2 diabetes. *Diabetes Care*. 2016; 39:353–362. [PubMed: 26786577]

44. Henry RR, Murray AV, Marmolejo MH, Hennicken D, Ptaszynska A, List JF. Dapagliflozin, metformin XR, or both: initial pharmacotherapy for type 2 diabetes, a randomised controlled trial. *Int J Clin Pract.* 2012; 66:446–456. [PubMed: 22413962]

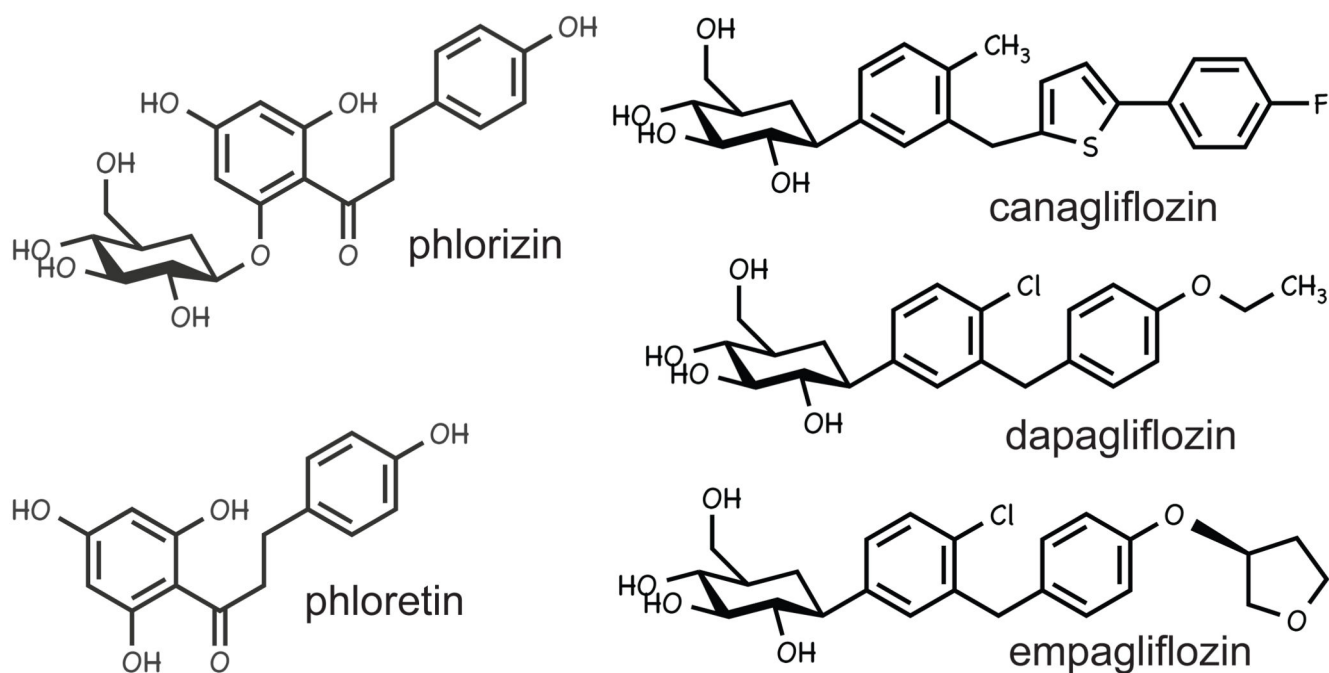


Figure 1. Structures of compounds used in this paper.

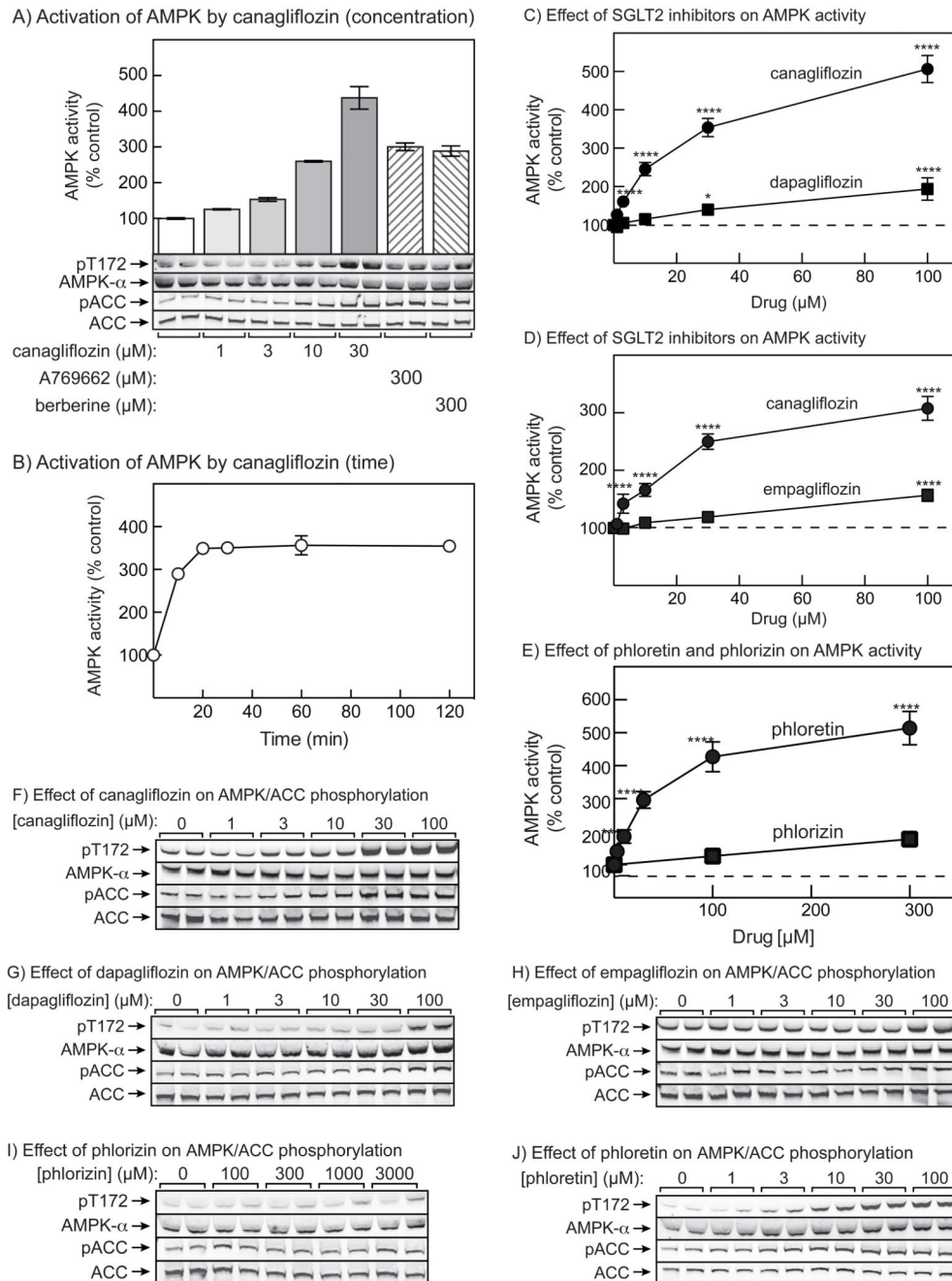


Figure 2. AMPK activation in HEK-293 cells by canagliflozin and other SGLT2 inhibitors. (A) HEK-293 cells were treated for 1 hr with the indicated concentrations of canagliflozin, or A769662 or berberine as positive controls. The upper panel shows kinase assays of immunoprecipitates prepared using anti-pan α antibodies (mean \pm SD, $n = 2$). The lower panel shows analysis of AMPK and ACC phosphorylation by Western blotting from duplicate dishes of cells. (B) Time course of AMPK activation by 30 $\mu\text{mol/l}$ canagliflozin (mean \pm SD, $n = 2$). (C) Comparison of effects of canagliflozin and dapagliflozin (1 hr incubations, mean \pm SEM, $n = 4$; significance of differences from DMSO controls

indicated). (D) Comparison of effects of canagliflozin and empagliflozin, as in (C). (E) Comparison of effects of phloretin and phlorizin, as in (C). (F)-(J) Phosphorylation of AMPK and ACC in duplicate wells in response to: (F) canagliflozin (from experiment in 2C); (G) dapagliflozin, from experiment in 2C; (H) empagliflozin, from experiment in 2D; (I) phloretin, from experiment in 2E; (J) phlorizin, from experiment in 2E. See Fig. S1 in Supplementary data for quantification of these blots.

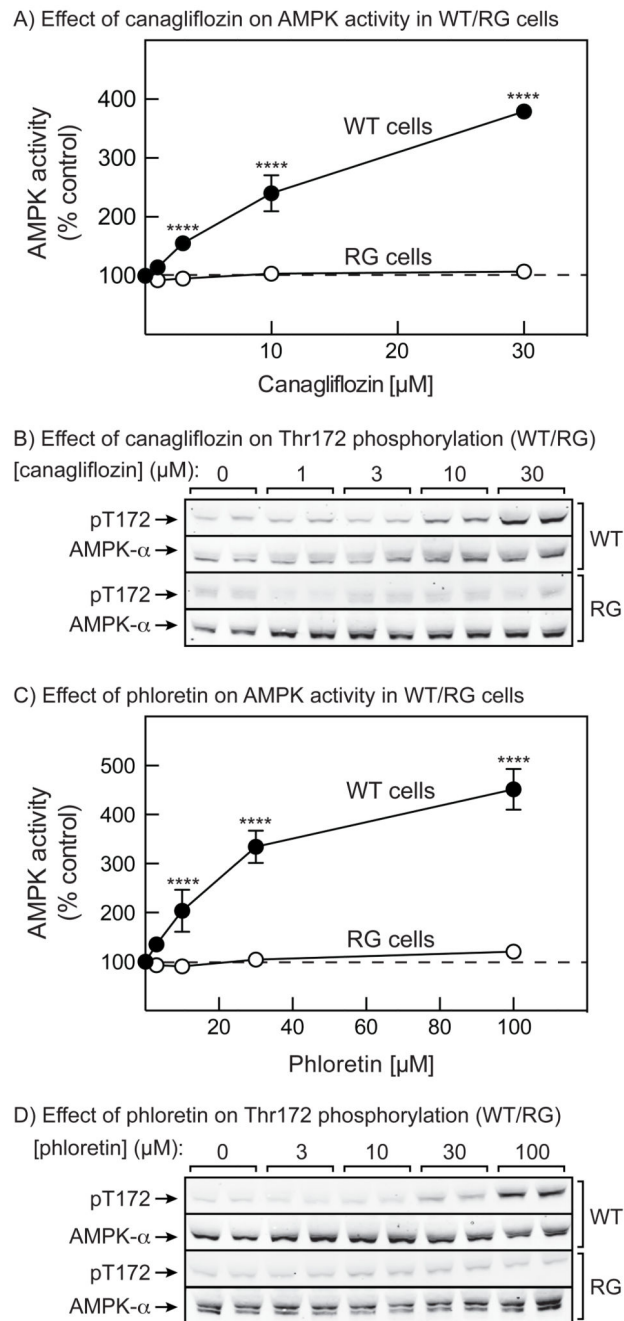


Figure 3. Comparison of AMPK activation by canagliflozin and phloretin in WT and RG cells. (A) WT and RG HEK-293 cells were treated for 1 hr with the indicated concentrations of canagliflozin, and the results of kinase assays in anti- α -immunoprecipitates are shown (mean \pm SEM, n = 4 to 6). Significance of differences from vehicle control are indicated. (B) Analysis of AMPK phosphorylation in duplicate dishes of cells from the same experiment as in (A). (C) As (A), but using phloretin. (D) As (B), but using phloretin. See Fig. S2 in Supplementary data for quantification of these blots.

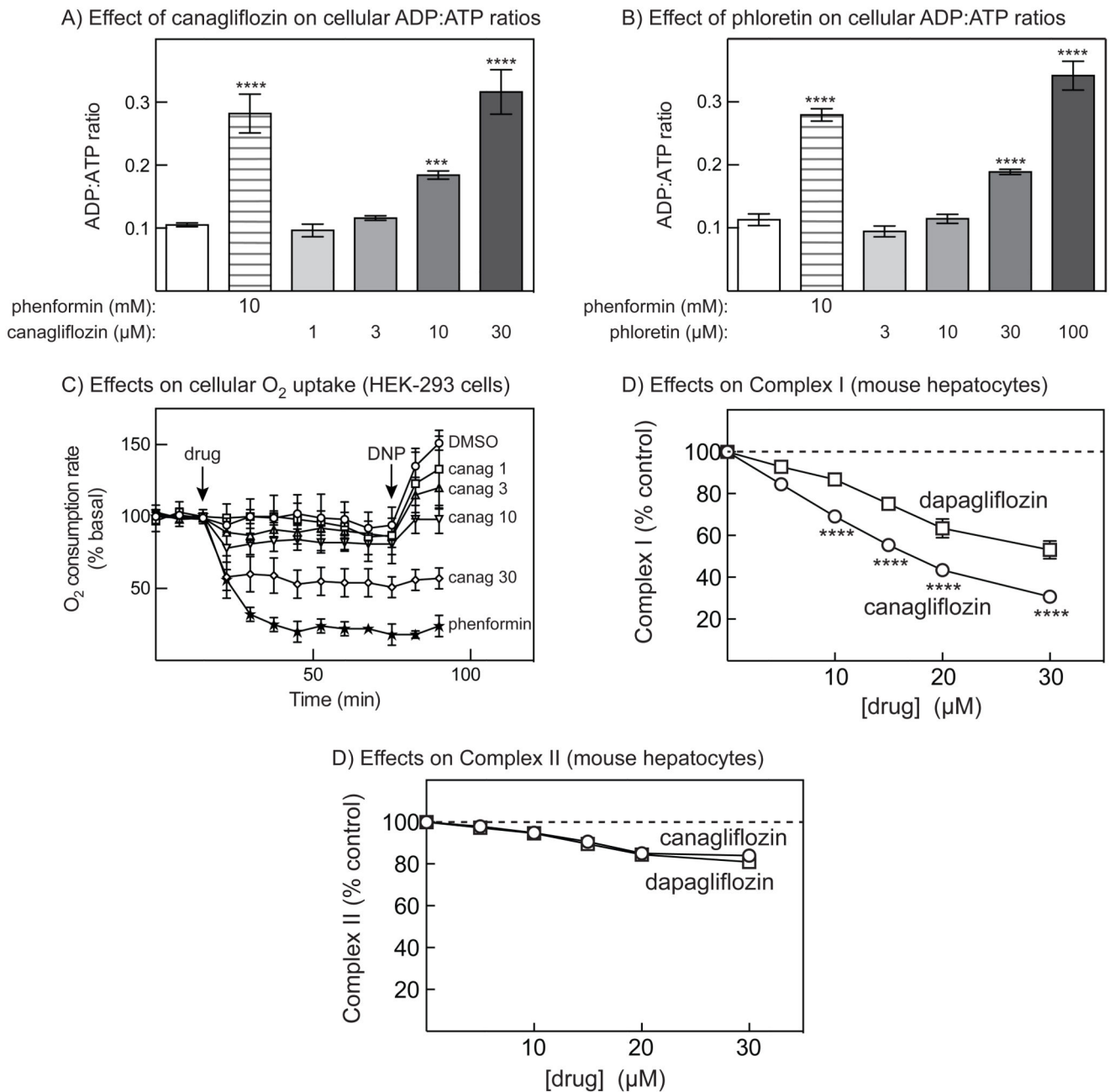


Figure 4. Effects of canagliflozin, phloretin and phenformin on cellular ADP:ATP ratios and oxygen uptake.

(A) Effects of phenformin and increasing concentrations of canagliflozin on cellular ADP:ATP ratios. HEK-293 cells were treated with the indicated drug concentration for 1 hr and cellular ADP:ATP ratios determined by capillary electrophoresis of perchloric acid extracts (mean \pm SEM, $n = 4$). Significances of differences from vehicle control are indicated. (B) As (A), but using phloretin in place of canagliflozin. (C) Effects of phenformin and increasing concentrations of canagliflozin on cellular oxygen uptake. At the point shown by the first arrow (“drug”) vehicle (DMSO), phenformin (10 mmol/l) or the

indicated concentration of canagliflozin ($\mu\text{mol/l}$) was added and oxygen uptake then measured at regular intervals. At the point shown by the second arrow (“DNP”) 2-dinitrophenol was added and oxygen uptake measured for a further 15 min. Results are expressed as % of the mean of the first 3 time points prior to drug addition (mean \pm SD, 3 replicate dishes performed twice, $n = 6$). After addition of drugs, the effects of 10 $\mu\text{mol/l}$ canagliflozin were significantly different from the DMSO control by 2-Way ANOVA (Dunnett’s multiple comparison test) at all time points except 67.5 and 75 min; effects of 30 $\mu\text{MOL/L}$ canagliflozin and 10 mmol/l phenformin were significant at all time points. (D)-(E) Complex I and II-supported respiration in permeabilized primary mouse hepatocytes. The cells were permeabilized with digitonin and then provided with ADP and glutamate and malate to stimulate Complex I-supported respiration, or rotenone, succinate and ADP to simulate Complex II-supported respiration. Results are expressed as percent inhibition of Complex I and II by canagliflozin and dapagliflozin (mean \pm SEM, $n = 3-5$). Statistically significant differences between effects of canagliflozin and dapagliflozin by 2-way ANOVA are indicated.

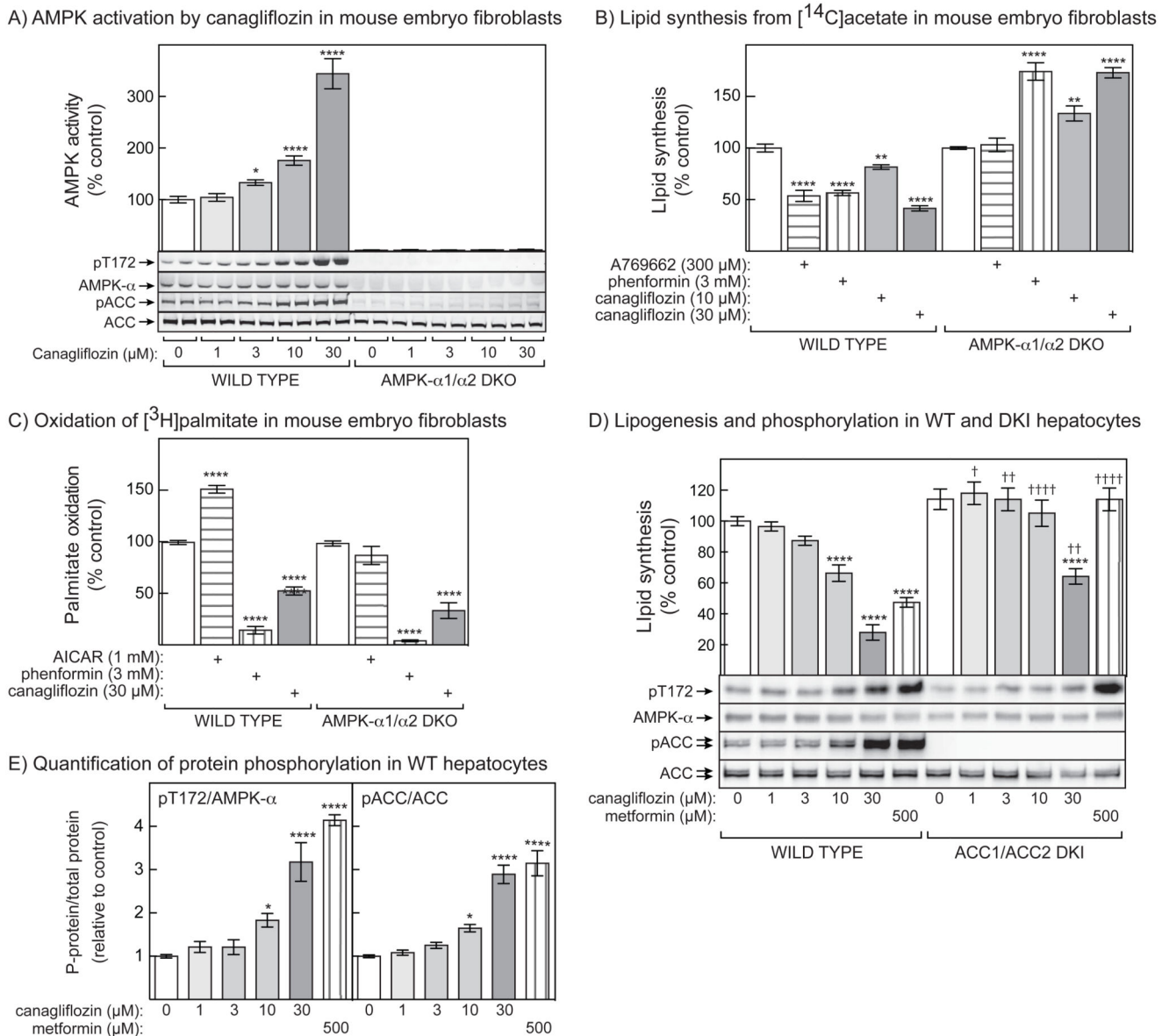
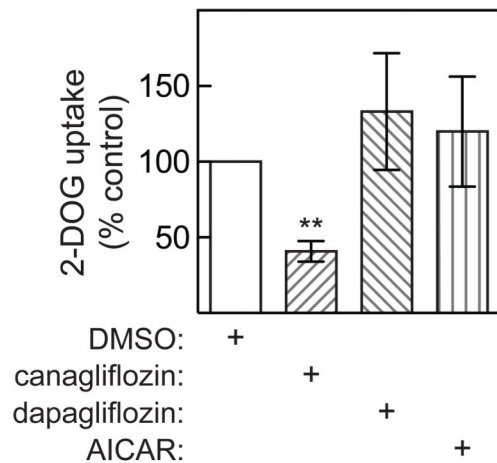


Figure 5. Effects of canagliflozin on AMPK, lipid synthesis and fatty acid oxidation in intact cells.

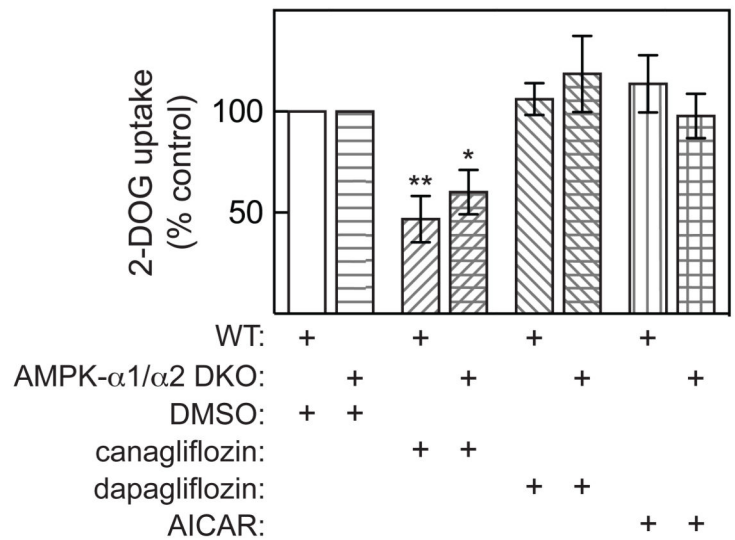
(A) Wild type and AMPK- $\alpha 1^{-/-}$ $\alpha 2^{-/-}$ MEFs (AMPK- $\alpha 1/\alpha 2$ DKO) were incubated with the indicated concentrations of canagliflozin for 1 hr and AMPK activity determined (upper panel) in anti-AMPK- α immunoprecipitates (mean \pm SEM, $n = 4$; assays were performed in the DKO cells although the activity, as expected, was negligible). Significance of differences from the vehicle control are indicated. The lower panel shows phosphorylation of AMPK and ACC analyzed in duplicate dishes of cells from the same experiment: see Fig. S3 in Supplementary data for quantification of these blots. (B) Lipid synthesis (incorporation of radioactivity from [¹⁴C]acetate into total lipid, i.e. fatty acids and sterols) in wild type and AMPK- $\alpha 1/\alpha 2$ DKO MEFs incubated in the indicated concentrations of A769662, phenformin or canagliflozin for 1 hr (mean \pm SEM, $n = 4$). Significance of differences from

vehicle controls are indicated. (C) Fatty acid oxidation (incorporation of radioactivity from [³H]palmitate into ³H₂O) in wild type and AMPK- α 1/ α 2 DKO MEFs incubated in the indicated concentrations of phenformin, AICAR or canagliflozin for 1 hr. Results are mean \pm SEM, n = 4; significance of differences from vehicle controls are indicated. (D) Lipid synthesis and protein phosphorylation in primary mouse hepatocytes from wild type and ACC1/ACC2 DKI mice. The upper panel shows incorporation of radioactivity from [³H]acetate into total lipid measured after 4 hr (mean \pm SEM, cells from 3 mice, each performed in triplicate). Significant differences from control within each genotype (**** P <0.0001) and between genotypes at the same drug concentration ($\dagger P$ <0.05, $\dagger\dagger P$ <0.01, $\dagger\dagger\dagger P$ <0.0001) are indicated. The lower panel shows analysis of protein phosphorylation by Western blotting of a representative example. (E) Quantification of the increases in phosphorylation in wild type hepatocytes of Thr172 on AMPK (left) or Ser79 plus Ser212 on ACC1/ACC2 (right), normalized for the expression of total AMPK or ACC1/ACC2 and expressed relative to control (mean \pm SEM, n = 4 for pT172/AMPK- α and n = 5 for pACC/ACC). Significant differences from vehicle controls are indicated.

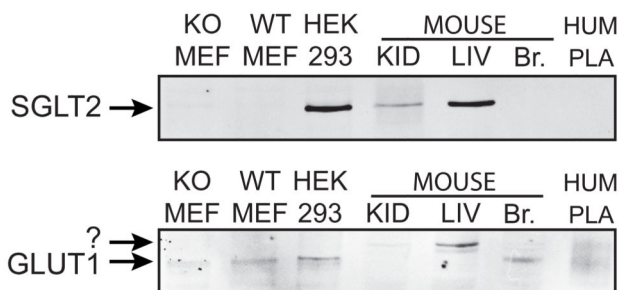
A) 2-Deoxyglucose uptake (HEK-293)



B) 2-Deoxyglucose uptake (MEFs)



C) Expression of glucose transporters



D) Effect of glucose removal (HEK-293)

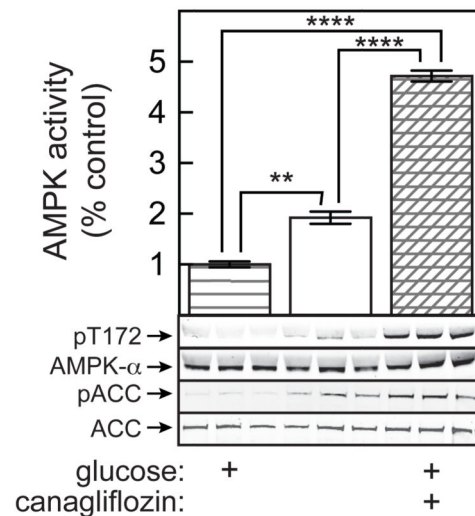


Figure 6. Canagliflozin inhibits glucose transport in HEK-293 cells and MEFs, but this does not account for AMPK activation.

(A) Uptake of 2-deoxyglucose (2DG) in HEK-293 cells treated with 10 $\mu\text{mol/l}$ canagliflozin, 10 $\mu\text{mol/l}$ dapagliflozin or 1 mmol/l AICAR. Results are mean \pm SEM ($n = 5$); significance of differences from vehicle controls are indicated. (B) As (A), but in wild type or AMPK- $\alpha 1^{-/-}/\alpha 2^{-/-}$ (DKO) MEFs. (C) Expression of SGLT2 and GLUT1; membrane fractions from MEFs or HEK-293 cells (80 μg protein), mouse kidney or liver (30 μg), mouse brain (15 μg) or human placenta (7.5 μg) were analysed by Western blotting and probed using the indicated antibodies. (D) Effect of total removal of medium glucose (centre) or 30 $\mu\text{mol/l}$ canagliflozin (right) on AMPK activity (top) and phosphorylation of AMPK (pT172) and ACC (pACC). Results in the bar chart are mean \pm SEM ($n = 3$); statistical significance of differences are indicated.

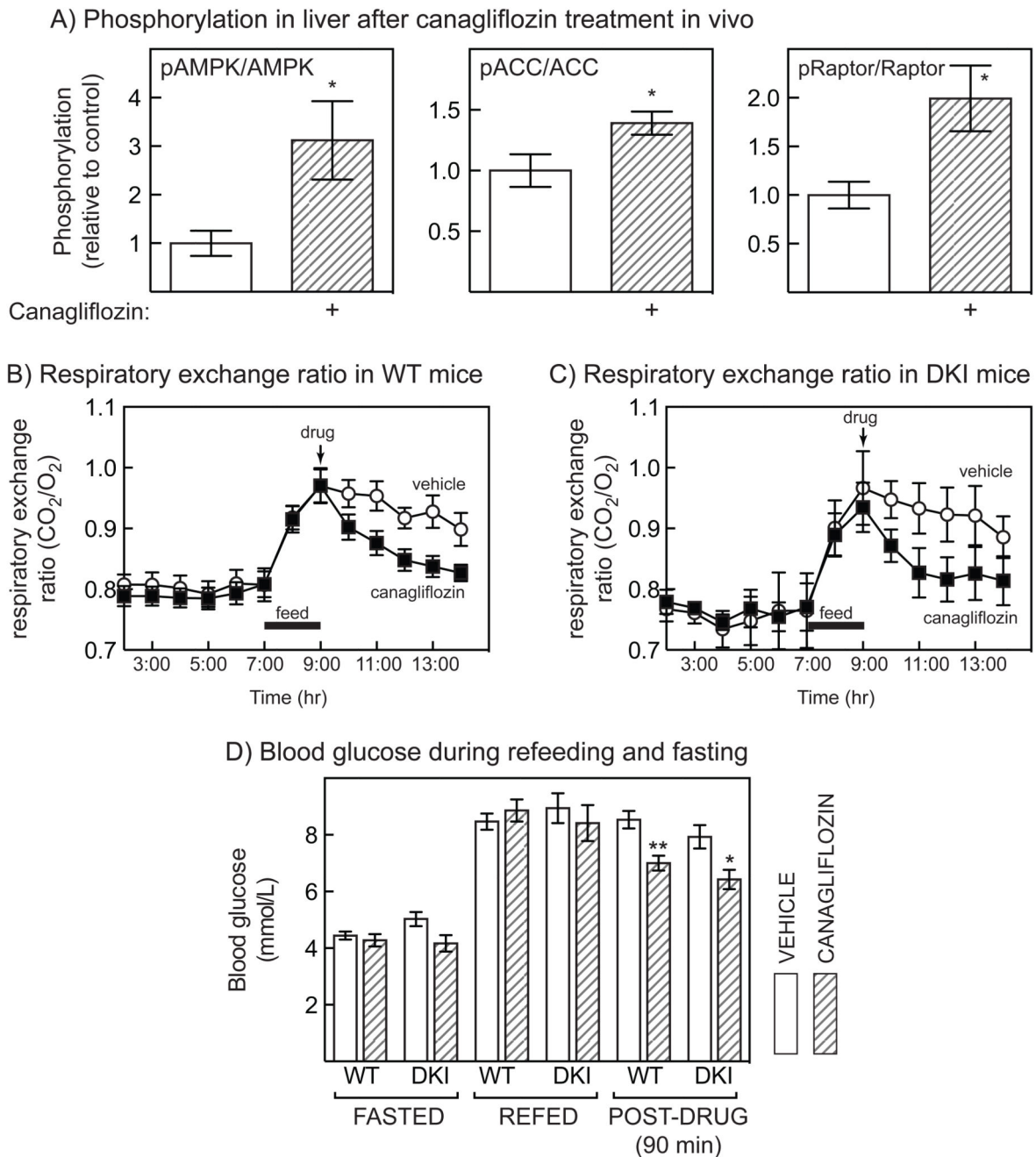


Figure 7. Liver AMPK is activated by oral administration of canagliflozin in mice, but this does not explain changes in respiratory exchange ratio.

(A) Phosphorylation of AMPK, ACC and Raptor relative to total protein in mouse liver after oral administration of canagliflozin (100 mg/kg) to mice. (mean \pm SEM, n = 9-11, significance of differences by Student's t test indicated). (B) Respiratory exchange ratio (CO_2/O_2) in 12 hr fasted mice that had been refed a carbohydrate-rich diet for 2 hrs between 7 and 9 am (black bars) and were then administered vehicle) or canagliflozin (30 mg/kg) at the time that food was withdrawn again. Results are mean \pm SEM, n = 10-12. (C) As (B), but experiments performed in ACC1/ACC2 DKI mice; results are mean \pm SEM, n = 5-7. (D)

Glucose concentrations in the tail vein during experiments of the type shown in Figs. 7B/C. Statistically significant differences in canagliflozin samples versus vehicle control are indicated.